Silicon (2019) 11:2873–2884
https://doi.org/10.1007/s12633-019-0070-y

ORIGINAL PAPER

Traveling Wire Electrochemical Discharge Machining (TW-ECDM) of Quartz Using Zinc Coated Brass Wire: Investigations on Material Removal Rate and Kerf Width Characteristics

Ankit D. Oza[1] · Abhishek Kumar[1] · Vishvesh Badheka[1] · Amit Arora[2]

Received: 28 August 2018 / Accepted: 7 January 2019 / Published online: 25 January 2019

Abstract
In this era, advanced non-conducting materials are gaining importance due to their superior properties. However, it is difficult to micro-machine these materials inefficiency and also economically still persists with currently used advanced non-traditional machining processes. Non-traditional machining processes are typically unfeasible for quartz material owing to its properties such as high strength, high melting point, high temperature-resistance, chemical stability and brittleness. Traveling wire electrochemical discharge machining (TW-ECDM) process is newly developed non-traditional machining process and has great potential for machining of quartz ceramics. Coated wire has been used to reduce the wire breakage and improves the efficiency. The input important input parameters have been selected for this process as applied voltage, electrolyte concentration and wire speed. Taguchi robust design was perform to identify the optimal parametric conditions using L_9 orthogonal array. Signal to noise (S/N) ratio and ANOVA were used to find the optimal parametric conditions and relative contribution of the input parameters respectively. Also, the surface finish was analyzed by scanning electron microscope (SEM). First time, coated wire with diameter of 0.15 mm has been used during TW-ECDM process. These obtained results present in this article will provide new guidelines to the micro-manufacturers, engineers and researchers.

Keywords TW-ECDM · Micro-machining · Quartz · Coated wire · MRR · K_w

1 Introduction

In recent era, the development of advanced engineering non-conducting materials like glass, ceramics, polymers, composites, fiber-reinforced plastic (FRP) etc. have tremendous applications in glass, foundry, optical, polymers, electronics components, aerospace and defese industries, micro electro mechanical system (MEMS) and bio-medical parts which are highly sophisticated [1].

Different non-traditional machining processes like water and abrasive jet machining, laser beam machining (LBM), ultrasonic machining (USM), ion beam machining (IBM) and electron-beam machining (EBM) are used to machine the non-conducting material. These processes are contactless and removal of the materials from the work-piece is done directly. Numerous kinds of physical and chemical energies are utilized to attain required shape, size, and precision. LBM has some material restrictions and chances of metal burning. USM has low material removal rate, high heat affected zone, high tool wear and larger grain size which causes defects. IBM and EBM need vacuum environment and also have low material removal rate for the machining. The equipment and machining cost of these processes are higher as compared to the suggested process. Additionally, these processes consume high power [2].

As far as the material removal rate, accuracy, and machining capabilities are concerned, two most popular non-traditional machining processes viz. electrochemical

✉ Ankit D. Oza
ankit.ophd15@sot.pdpu.ac.in

Abhishek Kumar
Abhishek.K@sot.pdpu.ac.in

Vishvesh Badheka
Vishvesh.Badheka@spt.pdpu.ac.in

Amit Arora
amitarora@iitgn.ac.in

[1] Pandit Deendayal Petroleum University, Gandhinagar 382007, India

[2] Indian Institute of Technology, Gandhinagar 382424, India

machining (ECM) and wire-electro discharge machining (W-EDM) have the maximum potential. But these processes have key limitations, i.e. these machines can work only on electrically conducting materials. To overcome the above-stated limitations, it is required to develop a machining process which can do micromachining of a variety of non-conducting materials, irrespective of strength, conductivity, brittleness, thickness, and hardness. Combination of above stated non-traditional machining processes can adequately use the benefits of each machining method and attain improved results than a sole method. If equipment can be constructed for all of these machining methods, it can act as multi-utility equipment and can be used appropriately with low cost and smaller working space constraints. Thus, it can be used efficiently for research combing effects for various kinds of energy and methods.

The electrochemical discharge was firstly developed by Kurafuji and Sudakin in 1968 and was termed as electrical discharge drilling. [3]. The electrochemical discharge machine (ECDM) is a mixture of two different non-traditional machining processes which is electrochemical machining (ECM) and electric discharge machining (EDM) [4]. The ECDM process is set up to be incredibly useful for the machining of advanced non-conducting materials having higher hardness and brittleness which are found to be difficult in machining. Electrochemical discharge machining (ECDM) is an upcoming micromachining technique with immense potential of fabricating micro-holes and micro-channels in different non-conductive hard and brittle materials.

However, ECDM itself has some limitations like low aspect ratio, limiting depth and low accuracy [5]. To conquer such limitations, Tsuchiya et al. [6] introduced the process named electrochemical discharge machining and reported that it can be used for cutting of various non-conducting materials like ceramics and glass. Further studies by Jain et al. [7] coined the term as electrochemical spark machine. The first time, in year 1997 Ghosh et al. [8] established a relation between the machining process and the electrochemical discharge phenomenon. The first literature on the process was published in 2005 [9] and a remarkable number of studies on this process emerged thereafter.

TW-ECDM is a newly developed hybrid machining process which combines the characteristics of electrochemical machining (ECM) and wire-electro discharge machining (W-EDM). Micro-Machining/Slicing a variety of non-conducting materials can be possible without removing a large amount of material by this process. Set-up and maintenance costs are very low as compared to other non-conventional processes [10].

The schematic diagram of the TW-ECDM process is shown in Fig. 1. This process is also known as traveling wire- electrochemical spark machining (TW-ECSM). Literature reveals that the material removal rate of TW-ECDM process can be 5 to 50 times higher than that of EDM and ECM and also decreases the electrode tool wear [10]. Moreover, this machining process is more stable than wire-electric discharge machining (W-EDM) and a better surface finish is obtained by electrochemical machining (ECM) [7, 9, 11].

The material removal mechanism is a high-temperature etching process. The material removal takes place by electro spark erosion (ESE) which helps machine of the workpiece and electrochemical dissolution (ESD) effect followed by the production of smooth surfaces [3–9, 12]. In TW-ECDM process there are two electrodes used and both are submerged in conducting electrolyte (alkaline or acidic). One of the electrodes is tool electrode i.e. cathode (circulating wire), which is used in slicing work-piece and the other is passive or a counter electrode, also known as an auxiliary electrode made of an anode. The continuously circulating wire electrode (cathode) is always touching with the workpiece. The auxiliary electrode (anode) is kept partially dipped in the electrolyte. To maintain current density at cathode, the auxiliary electrode is kept away from the tool-electrode about 20–50 mm. An electrolyte tank contains a suitable electrolyte. Additionally, appropriate fittings are provided to hold the work-piece. Direct current (DC) supply or Pulse (DC) supply is applied between the electrodes.

As the applied voltage increases the formation of gas bubbles increases followed by the increase in their mean radius. These gas bubbles are responsible for producing sparking effect, which turns into minute gas bubbles. Beyond the critical voltage, the bubbles collapse and form a gas layer around the tool electrode (wire). This gas layer acts as the barrier in between these two electrodes (anode and cathode). This facilitates the ionization of this layer and if the potential difference is sufficient for a given pair of the tool (wire) and electrolyte system, sparking is observed between electrode and electrolyte. This spark causes a streamlined stream of electrons to move with a very high velocity and acceleration from the wire towards the work-piece. This creates compressive shock waves on the workpiece surfaces which helps in removing material from these work-piece (non-conducting) in the form of melting, vaporization and thermal erosion as it happens in EDM [4, 5, 7–10, 13, 14].

From the literature review, it is found that researchers already worked on electrochemical discharge machining (ECDM) and traveling wire electrochemical discharge machining (TW-ECDM) processes. Some of the published research works are explained here in brief. Gautam and Jain investigated on ECDM by using different tool kinematics to improve the process performance [15]. Kulkani et al. [16] observed the discharge mechanism by different experimental conditions and projected the basic material removal mechanism. Panda and yadava estimate and studied the temperature field and material removal rate (MRR) by developed a 3-D

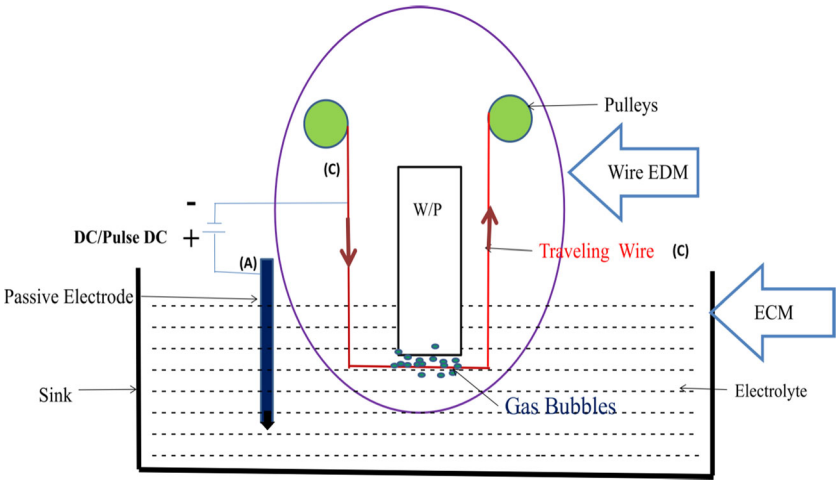

Fig. 1 Traveling wire electrochemical discharge machining (TW-ECDM) process

finite element transient thermal model [17]. Parametric analysis was done by manna and kundal of the TW-ECSM setup on material removal and spark gap width [18]. Back steeping analysis was done by suqin he et al. [19] to find out the combined effect of physical removal and chemical removal of ZrO2 ceramics. A considerable increment in the MRR can be possible by adding inductance observed by the Basak and Ghosh [20]. Yung et al. [21] shows that by adding SiC abrasive particle into the over cut quality, roughness and MRR in TW-ECDM process. Also study the effect of different parameters on process performance. Reduction of machining timing and the dreg discharge can be possible by the use of magnetic assistance in electro-chemical micro-machining and also improves the surface of the workpiece [22]. Magneto hydrodynamic approach improves the electrolyte movement in the machining gap. Also found that the MRR is increasing from 9.09 to 200% during process [23, 24].

It has also been observed that in W-EDM the use of coated wires gives better cooling ability and flushability compared to conventional wires. Also improves the good sparking ability, conductivity, productivity, strength without sacrificing fracture toughness [25]. Summary of already wire used in TW-ECDM process as shown in Table 1.

Above presented literature study reveals that the attempts made improve the process performance and various approaches has been used to reduce the wire breakage which include adding surfactant in electrolyte, electrode rotation, magnetic field and ultrasonic vibrated electrolyte. In the present research work, first time a zinc coated brass wire having diameter 0.15 mm is used to study the effect of different process parameters on TW-ECDM process. Zinc coated brass wire have a good cutting speed over the plain brass wire. And also improves the surface finish of the machined workpiece. Table 1 shows the different tool wire was used during TW-ECDM process.

In this study, a wire traveling wire electrochemical discharge machining (TW-ECDM) system has been developed and utilized to conduct experimental investigation of non-conductive quartz material. Innovations in the computers, consumer electronics, and communications (3C) industry, and electronics circuits as high quality tuned circuits or resonators, and the growing popularity of smart phones with touch screen functions have led to an increase in the demand for glass that is resistant against abrasion and scratch. Quartz seems to be an ideal candidate for such application. While quartz possesses good piezoelectric characteristics and has been widely applied in 3C products, there are machining challenges to overcome before quartz can be employed to fabricate touch screen. Being hard and brittle, quartz is difficult to machine. Traditional quartz machining which involves drilling, cutting, edging, polishing, thinning, laser engraving, and coating processes, produces machining stress, thus resulting in microcracks. Material properties of quartz are shown in Table 2.

2 Experimental Setup

Different micro-slicing tests were performed. This setup consists of main wire driving unit, electric supply unit, machining chamber, job holding unit, electrolyte tank, auxiliary electrode. Figure 2 shows the real in-house self developed TW-ECDM process.

1) Machining chamber unit:

Machining chamber is made of glass material due to its chemical resistivity, corrosion resistance and transparent properties. Size of chamber is 450 mm (L) × 150 mm (W) × 100 mm (H). This chamber contains the electrolyte. The auxiliary graphite electrode of round shape 20 mm diameter and 80 mm length is attached near to sparking zone. Perspex pulleys made of Teflon material are used to give smooth

Table 1 Summary of the tool wire used in TW-ECDM process

Authors	Wire material	Wire size (Diameter)	Workpiece material	Observations
Manna and Kundal [18].	Steel wire	0.070 and 0.090 mm	Al_2O_3 ceramic	Width of cut and surface finish reduced by selection of proper parameters
Yang et al. [21].	Brass wire	0.25 mm	Glass and quartz	Addition of SiC abrasive to electrolyte increases the critical voltage and reduces the discharge energy and slit expansion.
Rattan N. and Mulik R.S. [23].	Brass wire	0.1 mm	Quartz	MRR increases 9.09% to 200% under Magnetic field.
Rattan N. and Mulik R.S. [24].	Brass wire	0.1 mm	Quartz	MRR found more and discharge current is less under Magnetic field assisted TW-ECDM process.
Singh et al. [26].	Brass wire	0.50 mm	Zirconate Titanate	Melting and large cracks observed at higher voltage.
Liu et al. [27].	Molybdenum wire	0.18 mm	Al_2O_3 particle reinforced 6061 aluminum alloy	Reduction in MRR due to long pulses and presence of ceramic reinforcing phase from the machining gap.
Kuo et al. [28].	Brass wire	0.15 mm	Quartz	Better surface quality and machining precision achieved by SiC powder with titrated electrolyte flow
Singh et al. [29].	Zinc diffused brass wire	0.20 mm	Borosilicate glass	Wire breakage more at higher voltage and concentration.
Bhuyan and Yadava [30].	Brass wire	0.25 mm	Borosilicate glass	Surface finish and MRR improved under the different experimental conditions.
Mitra et al. [31].	Brass wire	0.25 mm	Hylam based composite	MRR, Surface roughness and Overcut improved by under the different experimental conditions.
Peng and Liao [32].	Stainless wire	0.25 mm	Optical glass, quartz and ceramic (Al2O3)	Voltage drop due to internal resistance of wire

Table 2 Material properties of quartz

Parameters	Description
Size	75(L)*25(W)*2(T) mm
Density	2.2×10^3 kg/m^3
Hardness	5.5–6.5 Mohs' Scale (N/mm^2)
Young's Modulus:	7.2×10^{10} Pa
Tensile Strength	50×10^7 Pa (N/m^2)
Coefficient of Thermal Expansion (20 °C–320 °C)	5.11×10^{-7} cm/cm °C
Thermal Conductivity (at 20 °C)	1.4 W/m °C

movement of wire and could maintained proper tension. The workpiece holding assembly is attached to centre and the upper body of the machining chamber.

2) Wire feeding control unit

A wire feeding control unit mainly consist of feed spool, donor and accepter pulleys and a steeper motor. Movement of the pulleys are controlled by the steeper motor. The input current and torque capacity of steeper motor is 2.8 A and 18 Kgcm respectively. The wire continuously travels at a constant speed (set by motor) towards the workpiece. The auxiliary electrode made of graphite is connected to the power supply and its distance from the workpiece is 20–60 mm.

3) Electrolyte tank

A rectangular shape glass chamber of the size 250 mm × 80 mm × 85 mm is fabricated to contain electrolyte during experiment. Depth gauge micrometer is used to measure the electrolyte level in the tank.

4) Power supply unit

Fig. 2 In-House developed TW-ECDM setup

The pulse DC power supply is used in the existing TW-ECDM setup. The selected range of applied voltage and current is 0-100 V and 6 A respectively. A positive terminal of power supply is given to the pulleys. And the negative terminal of power supply is connected with the auxiliary electrode (graphite rod).

3 Planning for Experiment

In the present study, two qualities such as material removal rate and kerf width have been optimized simultaneously during machining of quartz with hybrid approach of taguchi method and analysis of variance (ANOVA), F-test, and S/N ratio used. The analysis of parameters was done by the MINITAB software. The chosen influencing factors are input voltage (V), concentration of electrolyte (%) and the wire speed. To study the effect of different input process parameters viz. applied voltage, % of concentration and wire speed on material removal rate (MRR) and kerf width (Kw), taguchi robust L_9 (3^3) orthogonal array design were been used. Different factors and their levels are shown in Table 3. From the previous studies it has been observed that the traditional experimental design procedures are too complicated and not so easy to handle. A large number of experimental works have to be carried out when the number of process parameters are increased. To overcome this drawback, the Taguchi method was introduced which uses a special design of orthogonal arrays to study the entire parameter space with comparatively smaller number of experiments.

Taguchi methods have been widely utilized in engineering analysis and consist of a plan of experiments with the objective of acquiring data in a controlled way, in order to obtain information about the behaviour of a given process. The advantages of this method are saving of efforts in conducting experiments, saving experimental time, reducing the cost, and discovering significant factors quickly. Taguchi's robust design method is a powerful tool for the design of a high-quality system. In addition to the S/N ratio, a statistical analysis of variance (ANOVA) can be employed to indicate the impact of process parameters on response parameters.

Table 3 Table factors with levels

Factors	Levels		
	1	2	3
Voltage (V) (A)	30	35	40
Electrolyte Concentration (%) (B)	25	30	35
WIRE SPEED (m/min) (C)	3	8	13

The present analysis includes Taguchi method based parametric optimization technique to quantitatively determine the effects of various machining parameters on the quality characteristics of TW-ECDM process.

Applied voltage, electrolyte concentration and wire speed are the three input factors and each factor has three levels considered for the experiment. In the present study, the interaction between the input machining parameters are neglected. Based on the value of DOF = 8, it is concluded that at least 8 experiments are to be conducted to estimate the effects of each machining parameters. For the standard orthogonal array, at least three numbers of columns at three levels is selected. This array has total eight DOFs and it can handle four three-level input machining parameters. For orthogonal array matrix experiment, each machining parameter can be assigned to a column and nine-machining parameters combinations in L_9. Hence, only nine numbers of experiments are required to be conducted as per L_9, Since the L_9, orthogonal array has four columns, one column of the array is left empty for the error of experiments, and the orthogonality is not lost by letting one column of the array remain empty.

The selection of the range for input parameters were done on the basis of initial trial experiments and related literature. An initial trial was performed having different ranges as follows: Applied voltage (V) – 20 to 60 (V), Electrolyte Concentration (%) – 20 to 50 (%), wire speed – 0 to 15 (m/min). Based on initial trials, it was observed that the feasible ranges of Voltage (V) is – 30 to 40 (V), Electrolyte Concentration (%) is – 25 to 35 (%) and wire speed is – 0 to 15 (m/min). In the present research work, three levels of each machining parameters were selected as shown in Table 3.

In the present study, nine experiments were conducted having different parameters. For this Taguchi L_9 orthogonal array was used, which has nine rows corresponding to the number of tests, with three columns at three levels. L_9 orthogonal arrays (OA) have eight DOF, in which 6 were assigned to three factors (each one 2 DOF) and 2 DOF were assigned to the errors.

Parametric design of experiment is performed based on the selection of an appropriate standard orthogonal array. Signal-to-noise (S/N) ratio and ANOVA were carried out to study the relative importance of the machining parameters on both material removal rate (MRR) and Kerf Width (K_w) of TW-ECDM process for machining of quartz. Based on S/N ratio and ANOVA analysis, the optimal setting of the machining parameters for MRR and K_w were obtained.

The total degrees-of-freedom (DOFs) for experiments is calculated first to select an appropriate orthogonal array for the experiment. The applied voltage, electrolyte concentration and wire speed are the three factors and each factor has three levels considered for the experiment.

In Taguchi methodology, S/N ratio is used to measure the quality characteristics deviating from the desired value. The term signal represents the desirable mean value of the output

characteristics and the term noise represents the undesirable value (i.e., standard deviation) for the output characteristics. The S/N ratio (signal to noise) of each output characteristic has been studied. And finally, the analysis of variance (ANOVA) was used to find most significant parameter for the multiple responses. Analysis of variance (ANOVA) was performed to determine which machining parameter significantly affects the quality characteristics of the process and also to find the relative contribution of machining parameters in controlling the responses of the process.

The total sum of squared deviations SST from the total mean S/N ratio nm can be calculated as as shown in Eq. 1.

$$SS_T = \sum_{j=1}^{n} \left(n_j - n_m\right)^2 \quad (1)$$

Where n is the number of experiments in the orthogonal array and ηi is the mean S/N ratio for the ith experiment.

Degree of freedom (D.O.F.) has been calculated without considering the interaction effect among different control factors. D.O.F. due to grand total sum of squares = no. Of experiments = 9. Therefore D.O.F. due to total sum of squares = (9–1) = 8. But the D.O.F. for each factor = (3–1) = 2. Therefore D.O.F. for error = 8 - (2*3) = 2.

Percentage contribution of the process parameters on MRR and Kerf Width calculated as shown in equation no 2.

$$\%\text{Contribution} = \left(\frac{SS_d}{SS_T}\right) \quad (2)$$

Where, SS_d is the sum of the squared deviations.

F-ratio is a ratio of the mean square error to the residual error, and is traditionally used to Input determine the significance of a factor. It is calculated as shown in equation no 3.

$$\%\text{Contribution} = \left(\frac{SS_d}{SS_E}\right) \quad (3)$$

Where, SS_E is the sum of the square of error.

The material removal rate (MRR) was determined by using equation no 4.

$$\frac{\left(W_b - W_a\right)}{t} \quad (4)$$

W_b weight of workpiece before experiment (mg/min)
W_a weight of workpiece after experiment (mg/min)
t machining time (min)

Weight of the workpiece was measure by METTLER TOLEDO digital balance with accuracy 10 μg.

Kerf width (K_w) was determined by finding average of the difference between two corresponding points at three different places along the machined cut. Kerf width was measured by the scanning electron microscope (TESCAN – VEGA 3).

4 Results and Discussion

Taguchi robust design is used to determine the effect of each input parameters viz. voltage, electrolyte concentration and wire speed on MRR and Kerf width.

$$S/N = -10 \times \log\left(MSD\right) \quad (5)$$

Where, MSD is the mean square deviation.

In this present work, the values of S/N ratio were calculated for material removal rate (MRR) based on larger is better and for kerf width based on smaller is better. Equation 5 shows the calculation of S/N ration. The S/N ratios are given in Table 4 for MRR and K_w.

The analysis of variance (ANOVA) table for material removal rate (MRR) and kerf width (Kw) are shown in Tables 4 and 5 respectively.

4.1 Effects of Parameters on Material Removal Rate (MRR)

Figures 3 and 4 shows the variation of MRR vs Input Voltage (V). MRR increases as the input voltageincreases from 30 to 40 V, as presented in Figs. 3 and 4. The MRR is lowest at 30 V and highest at 40 V. As the applied voltage increases, the current density near machining zone also increases which further results in increasing the hydrogen gas bubbles. These bubbles generate a gas film insulation and thus the spark generation rate is also increased. Thereby, enhancing material removal rate. From Table 5, it can be observed that ANOVA of MRR, applied voltage is the most contributing (65.79%) process parameter of the process. ANOVA Table 5 also shows that the F-value of applied voltage is higher than the %

Table 4 Signal to noise (S/N) ratio

Experiment Nos.	Factor levels			Signal to noise ratio (S/N)	
	A	B	C	MRR	K_w
1	1	1	1	−13.535	−47.0779
2	1	2	2	−12.1496	−47.8970
3	1	3	3	−11.4243	−47.6288
4	2	1	2	−11.842	−47.1849
5	2	2	3	−9.50689	−47.5611
6	2	3	1	−8.94177	−47.6917
7	3	1	3	−10.1225	−48.0201
8	3	2	1	−7.97619	−47.5092
9	3	3	2	−7.29435	−47.5920

Table 5 ANOVA for material removal rate (MRR)

Factor	Degrees of freedom (DOF)	Sum of square (SS)	Mean square (MS)	F-Value	% age of contribution
1 (V)	2	0.029021	0.014511	39.20	**65.79830409**
2 (% Cons)	2	0.013885	0.006942	18.76	**31.48097764**
3 (Wire Speed)	2	0.000460	0.00230	0.62	1.042942003
Error	2	0.000740	0.000370		1.67777627
Total	8	0.044106			100.0000

concentration of electrolyte and wire speed. From the S/N ratio given by Fig. 4, it is observed that the optimal parametric combination for higher material removal rate (MRR) is $A_3B_3C_1$. Figure 5 shows the surface plot of two most contributing factors for MRR: voltage and % of Concentration.

Figures 3 and 4 shows the variation of % concentration of electrolyte vs MRR. MRR increases from 250 to 350 (g/L) with increase in % concentration of electrolyte (g/L). It was observed that MRR is lowest at 25% and highest at 35% of concentration. The increase in % concentration means conductivity of electrolyte is higher and form more chemical reactions. Hence the dissolution rate of ions also increases and high current density is observed at the tool electrode. With increase in the conductivity of electrolyte, the circuit current also increases which accelerate the electrolysis process and more hydrogen bubbles are produced at the machining zone. It increases the spark generation rate which results into a wide cut along the length of the workpiece. From the Table 5 ANOVA table of MRR, % concentration is second most contributing (31.48%) factor of the process.

Figure 3 shows the variation of wire speed vs MRR. MRR decreases with increase (3–13 (m/min)) in wire speed. Also, it is observed that the MRR is lowest at 13 m/min speed of wire. Wire speed plays vital role on material removal rate due to continuous and quick traveling of new wire across the machining zone which increases the crater formation rate and forms more spark per unit time. Hence the higher material removal rate is observed up to certain level of wire speed. However, at high traveling speed, spark does take place only at the bottom of the wire and thus lesser number of sparks were observed which reduces the material removal rate. From the ANOVA Table 5 of MRR, wire speed is lesser (third) contributing (1.0429%) factor of the process.

4.2 Effects of Parameters on Kerf Width (K_w)

Figures 6 and 7 shows the variation of wire speed vs K_w. K_w decreases with increase in wire speed from 3 to 13 (m/min). Also, its observed that the K_w is lowest at 3 m/min speed of wire. From the ANOVA Table 6 of K_w, wire speed is most contributing (20.17429%) factor of the process. Itstates that the effect of wire speed is highest on Kw. Wire speed has major effect on the Kerf width. As the wire speed increases, the electrolyte dissolution also increases. It is due to the fresh wire electrode coming quickly across the work piece and the sparking zone producing higher number of sparks per unit

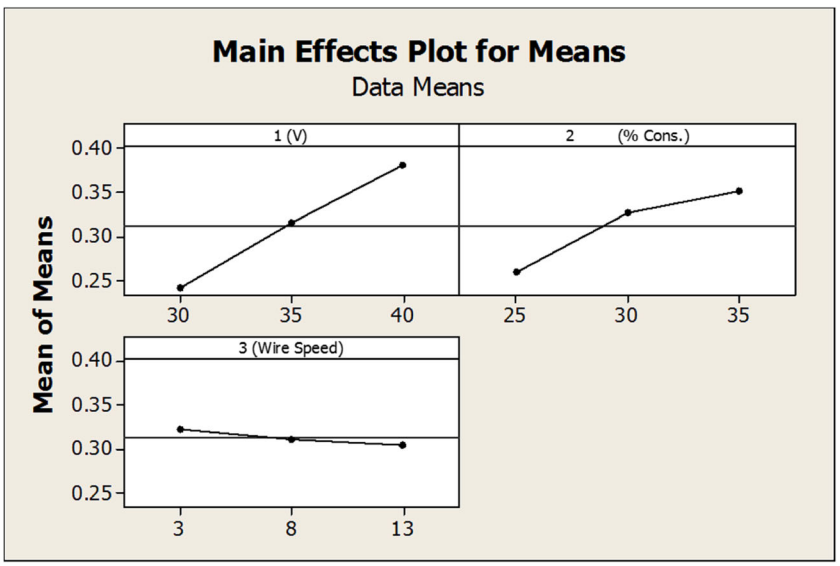

Fig. 3 Mean Effect plot for MRR

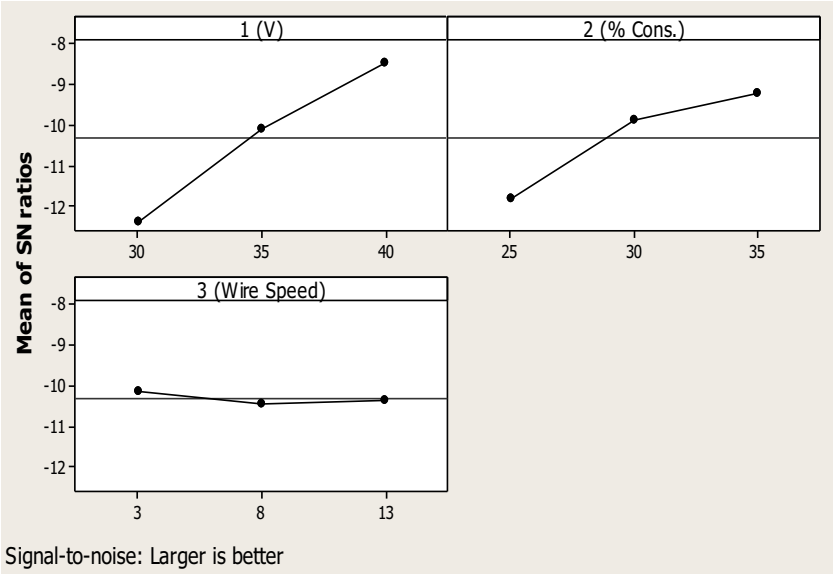

Fig. 4 S/N ratio plot for MRR

time. Hence higher material removal rate is observed. Also, the interaction time with workpiece is reduced resulting in lesser kerf width. From the S/N plot of Fig. 7, the optimal parametric combination for lower K_w is $A_2B_1C_1$.

Figures 6 and 7 shows the variation of % concentration of electrolyte vs K_w. $K_w$increases with an upsurge % concentration of electrolyte (g/L) from 250 to 350 (g/L). The Kw is the lowest at 25% and highest at 35% of concentration. Increase in electrolyte concretion (250–350 (g/L)) leads to an increase in circuit current followed by the sparking rate. As a result, higher amount of heat is generated which is responsible for higher material removal rate and higher Kerf width. Thus, the nature of the width of the cut is uneven. This drawback may be overcome by providing proper circulation of electrolyte and proper flashing of electrolyte. From the ANOVA Table 6 of K_w, % concentration is second most contributing (12.25%) factor of the process.

Figure 6 shows the variation of kerf width (K_w) vs Input voltage (V). K_w increases with input voltage from 30 to 40 V, as presented in Fig. 6. The Kw is lowest at 30 V and highest at 40 V. As the applied voltage increases, the rate of hydrogen gas bubbles also increases,

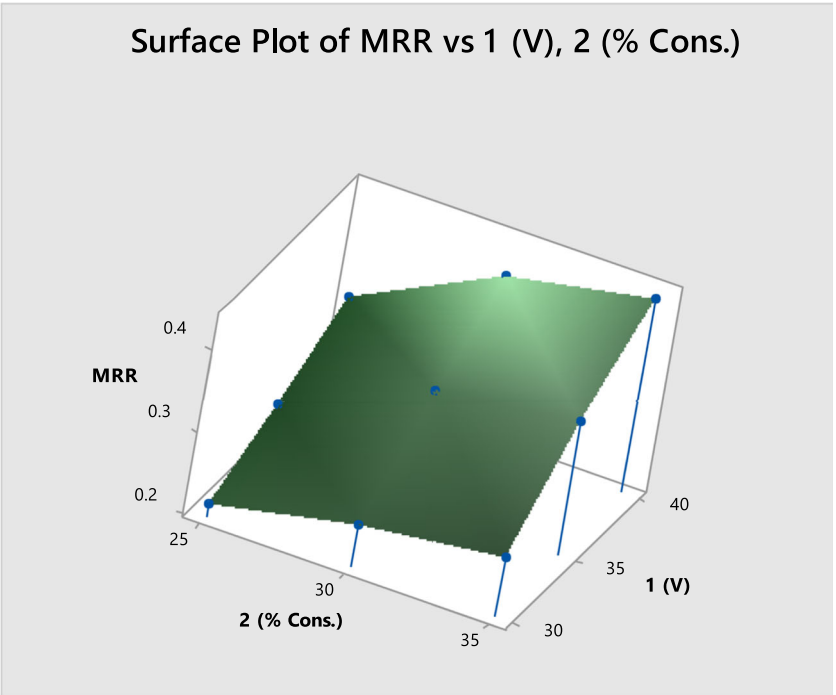

Fig. 5 Surface plot for MRR

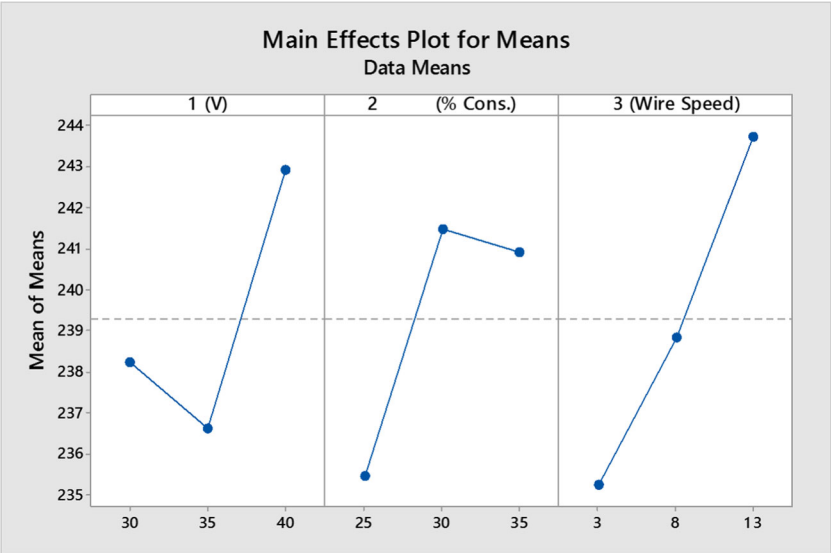

Fig. 6 S/N plot for K_w

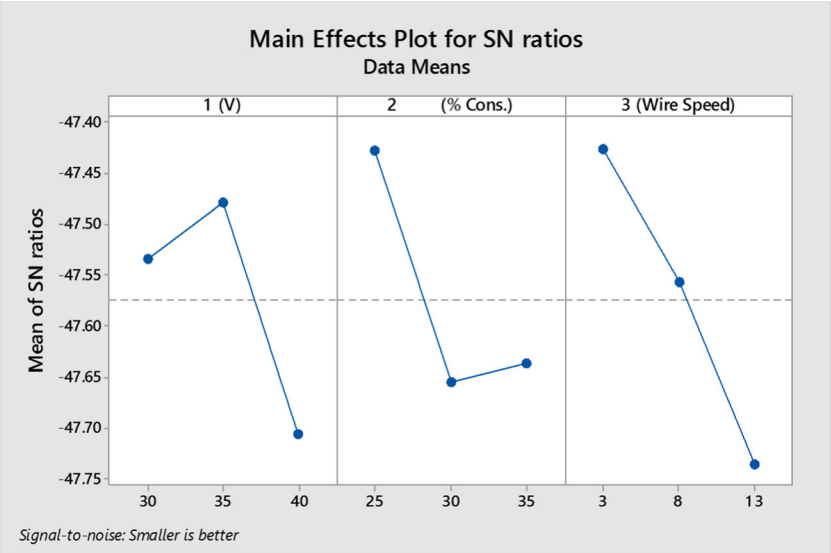

Fig. 7 S/N plot for K_w

resulting in large amount of sparking which can be observed at the machining zone. Thus, a higher amount of energy is responsible to melt the workpiece material. Also, some micro-cracks are observed due to high heat generation which results in high production of Kerf width. From the ANOVA Table 6 of K_w, applied voltage is the less contributing (11.80%) process parameter of the process. ANOVA Table no 6 also shows that the F-value of wire speed is lower than the % concentration of electrolyte and applied voltage. Figure 8 shows the surface plot of two most contributing factors for Kerf width (K_w): Wire speed and % of Concentration.

Table 6 ANOVA for Kerf width (Kw)

Factor	Degrees of freedom (DOF)	Sum of square (SS)	Mean square (MS)	F-Value	% age of contribution
1 (V)	2	64.15	32.08	0.21	11.80726
2 (% Cons)	2	66.58	33.29	0.22	12.25451
3 (Wire Speed)	2	109.61	54.8	0.36	20.17449
Error	2	302.96	151.48		55.761903
Total	8	543.31			99.999918

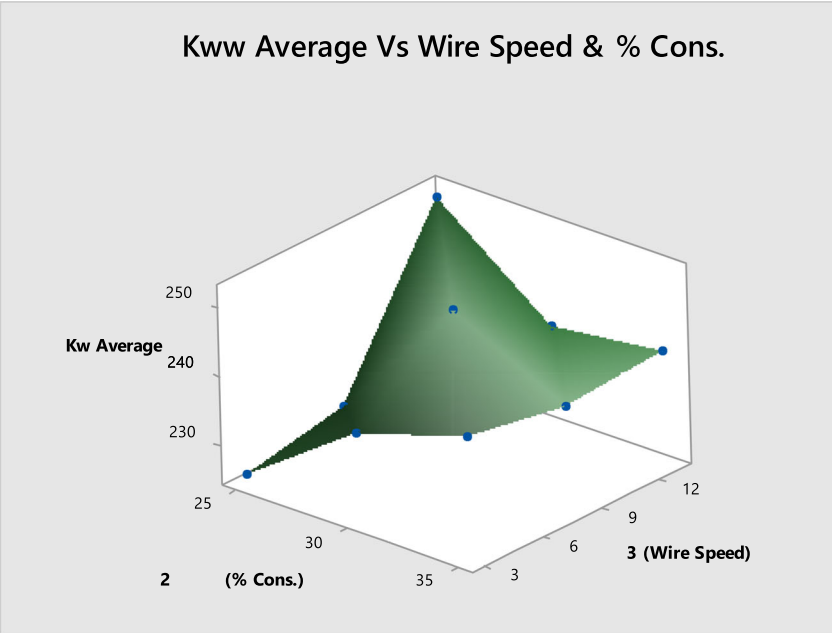

Fig. 8 Surface plot for K_w

5 Scanning Electron Microscope (SEM) Image Analysis

Figures 9 and 10 shows the SEM image of micro slice of quartz workpiece. Figure 9 shows the SEM image the results of continuous 10 min machining of quartz with 0.15 mm (diameter) zinc coated brass wire, input voltage 30 V, wire speed 3 m/min, 50 mm gap between wire and auxiliary electrode and 25% of concentration (250 g/L). And Fig. 10 shows the SEM image the results of continuous 10 min machining of quartz with 0.15 mm (diameter) zinc coated brass wire, input voltage 40 V, wire speed 13 m/min, 50 mm gap between wire and auxiliary electrode and 35% of concentration (350 g/L). In Fig. 9 some irregularities are observed as compared to Fig. 10 at the starting of the cutting side because of uneven flow of ions and less chemically dissolution strength of electrolyte. Also length of cut (LOC) is increases with increases applied voltage and concentration.

6 Conclusion

In the present work, hard and brittle and non-conducting quartz material has been machined using self-developed TW-ECDM setup. For the first time successfully used coated wire during the experiments. An experimental study has been carried out to analyze the effect of input process parameters

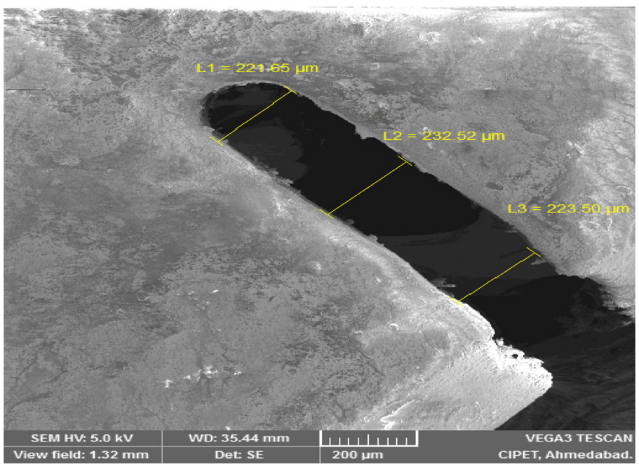

Fig. 9 SEM image

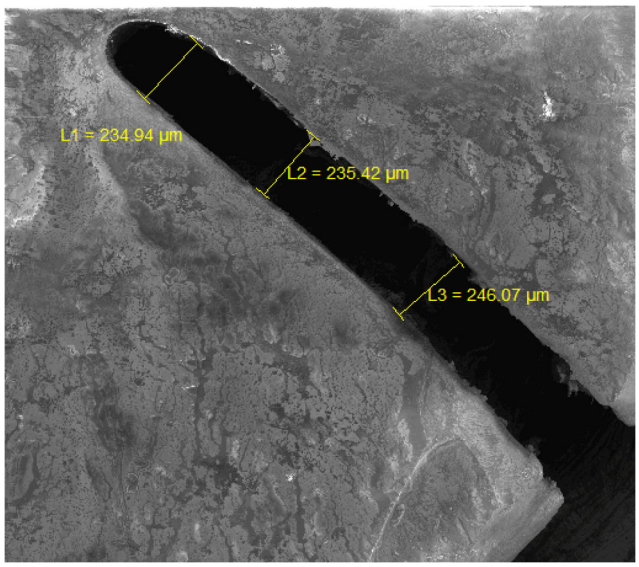

Fig. 10 SEM image

i.e. applied voltage (V), wire speed and (%) concentration on output parameters material removal rate (MRR) and Kerf width (K_w). Based on experiment following conclusions are summarized:

1) The self-house developed TW-ECDM setup can be successfully used for mico-machining/slicing of quartz material.
2) With the use of coated wire, significant hike in cutting speed is obtained. Over and above this, it affects the material removal rate in positive manner.
3) Coated wire gives better performance in terms of surface finishing and reduces the wire breakage phenomenon.
4) The performance characteristics in TW-ECDM process are mainly governed by the effects of voltage and % of concentration.
5) For higher material removal rate (MRR), high voltage and high % of concentration are recommended based on S/N ratio analysis. An ANOVA result also reveals that highest contributing (65.79%) of voltage in influencing the material removal rate. And second most contributing factor is % of electrolyte concentration (31.48%)
6) For lower Kerf width (K_w), Wire speed and % of electrolyte concentration are most recommended and significant parameters. An ANOVA results reveals that highest contributing factor is wire speed (20.17%) and second most is % of concentration 12.25%.
7) From the SEM Images, It was observed that the high surface roughness is mainly due to presence of craters. This could be possible due to the no flushing facility is provided during machining operation
8) From this experimental result, it is possible to micro-slicing of quartz material. The higher material removal rate, lower kerf width and surface finish can be achieved by proper selection of input parameters

Acknowledgments The authors are thankful to Office of Research and Sponsored Program (ORSP), Pandit Deendayal Petroleum University (P.D.P.U.), Gandhinagar - Gujarat, India for providing experimental facility and financial assistance to carry part of this research work under the project number: ORSP/R&D/SRP/2017/AOAK.

References

1. Judy JW (2001) Microelectromechanical systems (MEMS): fabrication, design and applications. Smart Mater Struct 10:1115–1134. https://doi.org/10.1088/0964-1726/10/6/301
2. Jia B, Wang ZL, Hu FQ, Li XH, Zhao WS (2004) Research on multifunctional micro machining equipment. Mater Sci Forum 471-472: 37–42. https://doi.org/10.4028/www.scientific.net/msf.471-472.37
3. Kurafuji H, Suda K (1968) Electrical discharge drilling of glass. Ann CIRP 16:415–418
4. Fascio V (2003) Investigations of the spark assisted chemical engraving. Electrochem Commun 5:203–207. https://doi.org/10.1016/s1388-2481(03)00018-3
5. Crichton IM, Mcgeough JA (1985) Studies of the discharge mechanisms in electrochemical arc machining. J Appl Electrochem 15: 113–119. https://doi.org/10.1007/bf00617748
6. Tsuchiya H, Inoue T, Miyazaki M (1985) Wire electro-chemical discharge machining of glasses and ceramics. Bull Jpn Soc Precis Eng 19-1:73–74
7. Jain VK (1991) Experimental investigations into traveling wire electrochemical spark machining (TW-ECSM) of composites. J Manuf Sci Eng 113:75. https://doi.org/10.1115/1.2899625
8. Ghosh A (1997) Electrochemical discharge machining: principle and possibilities. Sadhana 22:435–447. https://doi.org/10.1007/bf02744482
9. Wüthrich R, Fascio V (2005) Machining of non-conducting materials using electrochemical discharge phenomenon—an overview. Int J Mach Tools Manuf 45:1095–1108. https://doi.org/10.1016/j.ijmachtools.2004.11.011
10. Singh T, Dvivedi A (2016) Developments in electrochemical discharge machining: a review on electrochemical discharge machining, process variants and their hybrid methods. Int J Mach Tools Manuf 105:1–13. https://doi.org/10.1016/j.ijmachtools.2016.03.004.
11. Liu J, Yue T (2012) Electrochemical discharge machining of particulate reinforced metal matrix composites. Mach Technol Compos Mater. 242–65. https://doi.org/10.1533/9780857095145.2.242
12. Yang C, Ho S, Yan BH (2001) Micro hole machining of borosilicate glass through electrochemical discharge machining (ECDM). Key Eng Mater 196:149–166. https://doi.org/10.4028/www.scientific.net/kem.196.149
13. Goud M, Sharma AK, Jawalkar C (2016) A review on material removal mechanism in electrochemical discharge machining (ECDM) and possibilities to enhance the material removal rate. Precis Eng 45:1–17. https://doi.org/10.1016/j.precisioneng.2016.01.007
14. Malik A, Manna A (2017) Travelling wire electrochemical spark machining: an overview. Materials Forming, Machining and Tribology Non-Traditional Micromachining Processes 393–411. https://doi.org/10.1007/978-3-319-52009-4_11
15. Gautam N, Jain VK (1998) Experimental investigations into ECSD process using various tool kinematics. Int J Mach Tools Manuf 38: 15–27. https://doi.org/10.1016/s0890-6955(98)00034-0
16. Kulkarni A, Sharan R, Lal G (2002) An experimental study of discharge mechanism in electrochemical discharge machining. Int J Mach Tools Manuf 42:1121–1127. https://doi.org/10.1016/s0890-6955(02)00058-5
17. Panda MC, Yadava V (2009) Finite element prediction of material removal rate due to traveling wire electrochemical spark machining. Int J Adv Manuf Technol 45:506–520. https://doi.org/10.1007/s00170-009-1992-0
18. Manna A, Kundal A (2013) An experimental investigation on fabricated TW-ECSM setup during micro slicing of nonconductive ceramic. Int J Adv Manuf Technol 76:29–37. https://doi.org/10.1007/s00170-013-5145-0
19. He S, Tong H, Liu G (2018) Spark assisted chemical engraving (SACE) mechanism on ZrO 2 ceramics by analyzing processed products. Ceram Int 44:7967–7971. https://doi.org/10.1016/j.ceramint.2018.01.236
20. Basak I, Ghosh A (1996) Mechanism of spark generation during electrochemical discharge machining: a theoretical model and experimental verification. J Mater Process Technol 62:46–53. https://doi.org/10.1016/0924-0136(95)02202-3

21. Yang C, Song S, Yan B, Huang F (2006) Improving machining performance of wire electrochemical discharge machining by adding SiC abrasive to electrolyte. Int J Mach Tools Manuf 46: 2044–2050. https://doi.org/10.1016/j.ijmachtools.2006.01.006
22. Pa P (2009) Super finishing with ultrasonic and magnetic assistance in electrochemical micro-machining. Electrochim Acta 54:6022–6027. https://doi.org/10.1016/j.electacta.2009.01.063
23. Rattan N, Mulik RS (2016) Improvement in material removal rate (MRR) using magnetic field in TW-ECSM process. Mater Manuf Process 32:101–107. https://doi.org/10.1080/10426914.2016.1176197
24. Rattan N, Mulik RS (2018) Experimental set up to improve machining performance of silicon dioxide (quartz) in magnetic field assisted TW-ECSM process. Silicon 10:2783–2791. https://doi.org/10.1007/s12633-018-9818-z
25. Maher I, Sarhan AAD, Hamdi M (2014) Review of improvements in wire electrode properties for longer working time and utilization in wire EDM machining. Int J Adv Manuf Technol 76:329–351. https://doi.org/10.1007/s00170-014-6243-3
26. Singh YP, Jain VK, Kumar P, Agrawal DC (1996) Machining piezoelectric (PZT) ceramics using electro-chemical spark machining (ECSM) process. J Mater Process Technol 58:24–31
27. Liu JW, Yue TM, Guo ZN (2009) Wire electrochemical discharge machining of Al2O3 particle reinforced aluminum alloy 6061. Mater Manuf Process 24:446–453
28. Kuo KY, Wu KL, Yang CK, Yan BH (2015) Effect of adding SiC powder on surface quality of quartz glass microslit machined by WECDM. Int J Adv Manuf Technol 78:73–83
29. Singh A, Jawalkar CS, Vaishya R et al (2014) A study on wire breakage and parametric efficiency of the wire electro chemical discharge machining process. In: all India manufacturing technology, design and research conference, IIT Guwahati, 12th Dec.–14th Dec. 2014, Assam, p 6
30. Bhuyan BK, Yadava V (2014) Modelling and optimization of travelling wire electro-chemical spark machining process. Int J Ind Syst Eng 18:139–158
31. Mitra NS, Doloi B, Bhattacharyya B (2015) Predictive analysis of criterial yield during travelling wire electrochemical discharge machining of Hylam based composites. Adv Prod Eng Manag 10:73–86
32. Peng WY, Liao YS (2004) Study of electrochemical discharge machining technology for slicing non-conductive brittle materials. J Mater Process Technol 149:363–369